GEOMETRICALLY OPTIMAL SPHERE EVERSION

MEHANA ELLIS

Abstract. In this paper, we will look at the process of turning a sphere inside out, which is called *sphere eversion*. We will cover important topics in sphere eversion such as Smale's proof [Sma59] of the existence of crease-free sphere eversion, bending energy, minimax eversions, topological stages in the eversion, and more. Much of the content in this paper is based on the sphere eversion research of John M. Sullivan [Sul02], as well as Bednorz et. al. [BB19].

1. Introduction to Sphere Eversion and Smale's proof

The idea of sphere eversion is essentially turning the sphere inside-out, which is a continuous deformation because the sphere is never cut, torn, or creased in the process. This concept was first researched after Stephen Smale proved a theorem in his 1957 paper "A Classification of Immersions of the Two-sphere," which showed that this was possible. Some decades later, sphere eversion was further popularized by the 1998 video *"The Optiverse"*, which showed the process using minimax eversions. This diagram shows some steps of a sphere eversion:

Figure 1. Process of continuous sphere eversion.

Many interesting discoveries were made along the way to the geometrically optimal eversion process. We will begin by looking at Smale's indirect proof, which is based on regular homotopy classes of immersions of spheres. While this is a bit like jumping into the deep end, especially considering the difficulty of his paper, it will provide us with a chance to learn and review some definitions.

Definition 1.1. An *immersion* of a sphere (or any differentiable manifolds) is a differentiable function between two manifolds whose differential is injective everywhere.

Definition 1.2. A *turning number* of a closed curve around a point p is the number of times that the curve travels counterclockwise around p.

Date: June 6, 2022.

Knowing these definitions, we can now present a general idea of the Whitney-Graustein theorem.

Theorem 1.3 (Whitney-Graustein)**.** *Two immersions of a differentiable manifold are regularly homotopic if and only if they have the same turning number.*

Smale states that the Whitney-Graustein theorem classifies immersions of the circle S^1 in the plane E^2. Here is his own theorem, quoted directly from his paper.

Theorem 1.4 (Smale)**.** *If f and g are C^2 immersions of S^2 in E^n, they are regularly homotopic if and only if $\Omega(f, g) = 0$. Furthermore let $\Omega_0 \in \pi_2(V_{n,2})$ and let a C^2 immersion $f : S^2 \to E^n$ be given. Then there exists an immersion $g : S^2 \to E^n$ such that $\Omega(f, g) = \Omega_0$. Thus there is a 1-1 correspondence between elements of $\pi_2(V_{n,2})$ and regular homotopy classes of immersions of S^2 in E^n. [Sma59]*

Because we have $\pi_2(V_{3,2}) = 0$, Smale's theorem also yields the following theorem.

Theorem 1.5. *Any two C^2 immersions of S^2 in E^3 are regularly homotopic. [Sma59]*

While Smale's paper certainly provides more insights into the early studies of sphere eversion, we will now look at John M. Sullivan's more recent paper, which covers a wide range of modern research on the topic.

2. Bending Energy

Next, we will look at the means by which the sphere can be everted, namely *elastic bending energy*. Essentially, elastic bending energy (or simply, bending energy) assigns the integral of a square of the mean curvature to any immersed surface. It can also be thought of, in physics, as the mechanical potential energy stored in the object as it undergoes continous deformation. The actual release of this energy occurs when the object is deformed, e.g. when it is stretched.

A surface in space has two principal curvatures at each point, and squaring the integral of the mean curvature (the average of the principal curvatures) gives us the bending energy for surfaces. This is often referred to as the *Willmore energy*.

Note that out of all closed surfaces, it is the sphere which has minimal bending energy. We say that the sphere has energy 1.

Proposition 2.1. *Any self-intersecting surface with a k-tuple point has energy of at least k.*

In the case of a sphere, in order for the eversion to occur, the sphere must pass through a stage with a quadruple point, because the bending energy must be at least 4 for this to occur. [Sul02]

3. Topology of Eversion

When we invert a sphere, or more generally, when a generic regular homotopy occurs, there are topological "stages" which correspond with specific times in the deformation. For example, we can see such various stages of continuous sphere eversion in Figure 1, where it appears that the sphere gradually sinks into itself, then the inner layer (shown in yellow) appears and one possible eversion (in this case, "closed halfway") has occurred. Each stage

occurs when two sheets of the surface are tangent to each other, when three sheets with a shared tangent line intersect, or when there is a quadruple point at which four sheets congregrate. Note that in the first case, a double curve is created, ended, or reconnected by the two sheets. In any of these cases, the stages occur when the surface normals are linearly dependent at the intersection point.

4. Minimax Eversions

Let us now look at the geometrically optimal for everting a sphere. We can do this by minimizing the eversion's middle elastic bending energy in the following way. We begin with a round sphere, and push down the "north pole" through the "south pole," resulting in the first double-curve from self-intersection. This creates two bulge-like shapes, one on each side, and the second double-curve is obtained by pushing each bulge through the other. Triple points are then found where these double-curves cross over. As seen in the halfway model (fifth step in Figure 1), each of the four triple points congregate at the quadruple point. Therefore, this final result, the halfway model, is the geometrically optimal way to observe a sphere eversion.

5. The mathematics behind eversion

Now that we have a better understanding of the general topological processes which are happening to create the sphere eversion, let's now take a look at some of the actual mathematics behind a similar deformation, namely, cylinder eversion. We can picture a cylinder as a sphere with poles cut out of the top and bottom. However, rather than a cylinder with finite height, this cylinder is extended to infinity. Note that a sphere is denoted $\mathcal{S}^2$ in space $\mathbb{R}^3$. Let the cylinder be parametrized by $(h, \phi) \in \mathbb{R} \times \mathcal{S}^1$, where $\mathcal{S}^1$ is parametrized by a real variable of the period 2π. The immersion (as in Definition 1.1) is then

$$x = \sin(n-1)\phi - h\sin\phi, y = \cos(n-1)\phi + h\cos\phi, z = h\sin n\phi,$$

for a natural $n \geq 2$. This surface is always smooth.

We will now briefly look at orientability, an important concept in topological spaces.

Definition 5.1. We call a topological space *orientable* if we can assign a clear and constant definition of "clockwise" and "counter-clockwise." We refer to this property as *orientability*. Furthermore, a space is called *non-orientable* if "clockwise" becomes "counter-clockwise" after moving continuously along a loop.

In other words, if a shape is positioned on such a space, completes one loop, and is mirror-imaged or flipped, the space is non-orientable.

Example. A torus is an orientable surface. If a shape is positioned on the torus and completes a full loop, it will not appear mirror-imaged or flipped upon arrival to its starting position.

Example. A Möbius strip is a non-orientable surface. If a shape is positioned on the Möbius strip and completes a full loop, it flips right/left upon circulation when it arrives back to its starting position.

If n is odd in the latter immersion, then the mapping $h \to h$, $\phi \to \phi + \pi$ yields the same point, but the point is oriented oppositely. We had that $n = 2$ due to the period of 2π. Because this surface is symmetric, we can more easily examine it as a halfway model. However,

we will look at the case of $n = 3$, which has more interesting properties. We have that this surface (known as Boy's surface) can be closed at infinity. It is a smooth immersion of the real projection plane ($\mathcal{S}^2$) in $\mathbb{R}^3$, which is a sphere in $\mathbb{R}^3$. Boy's surface is non-orientable. It also has a single three-fold intersection at $(0, 0, 0)$ and trifolium self-intersection, and at $n = 3$, it is quintic (has degree 5).

Going back to the notion of "stages" of eversions, we have the following general time-dependent parametrizations for the surfaces:

$$x = t\cos\phi + \sin(n-1)\phi - h\sin\phi$$
$$y = t\sin\phi + \cos(n-1)\phi + h\cos\phi$$
$$z = h\sin n\phi - (t/n)\cos n\phi.$$

The latter is a result obtained by Bednorz et. al. [BB19] Now we can use these parametrizations for sphere eversion when $n \geq 2$. Although we learned about some exciting properties where $n = 3$, we still have plenty to examine in the case of $n = 2$. The $n = 2$ surface allows us to have an even more detailed view of what exactly is happening during the eversion process.

6. Understanding the Process

We will next look closer at the process of sphere eversion, illustrated in the following diagram from Bednorz et. al., created in Mathematica. [BB19]

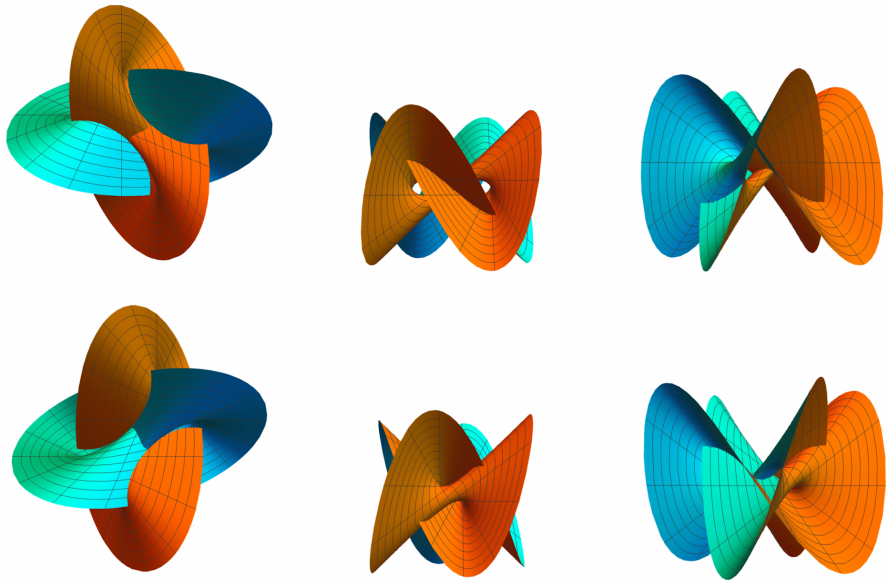

Figure 2. The halfway $n = 2$ surface at the points T_+ (top), and T_- (bottom), $t = \mp(\sqrt{17} - 3)/2$, the pairs being viewed from different angles.

On the bottom left, we see a surface with central point Q. The bottom middle depicts a pair of D_1 points. The bottom right shows a pair of D_1 points and another added D_1, Q, and the last D_1, which are all on a central perpendicular line. Note that $D_0 = D_2 = (0, 0, 0)$ at

$t = \pm 1$. The points denoted T_+ and T_- represent the birth/start (+) and death/end (−) of three-fold intersections, and they occur at $t = \pm(\sqrt{17} - 3)/2 \simeq \pm 0.56$. These t are at $z = 0$ and $x = -y = \pm(\sqrt{17} - 5)/2\sqrt{2}$ at T_+, and $x = y = \pm(\sqrt{17} - 5)/2\sqrt{2}$ at T_-.

With regard to the appearance of the $n = 2$ surface, when $|t| > 1$ it looks like a wormhole. Additionally, its self-intersections are simple. As the value of $|t|$ increases, the n-surfaces where n is substantially high still have simple self-intersections. This is due to the fact that the domain creates two embedded surfaces at $h = (n-1)\cos n\phi$. Concerning the full eversion, it is necessary for the surface to be free of self-intersections. Our time-dependent parametrizations for the surfaces in terms of stages, which we presented earlier, can now be generalized to the following:

$$\begin{aligned} x &= t\cos\phi + p\sin(n-1)\phi - h\sin\phi \\ y &= t\sin\phi + p\cos(n-1)\phi + h\cos\phi \\ z &= h\sin n\phi - (t/n)\cos n\phi - qth, \end{aligned}$$

where $q \geq 0$. Note that it is smooth for $(n-1)p(1-q|t|) + qt^2 > 0$. In the case that $n = 2$, it is sextic, as shown in Figure 3.

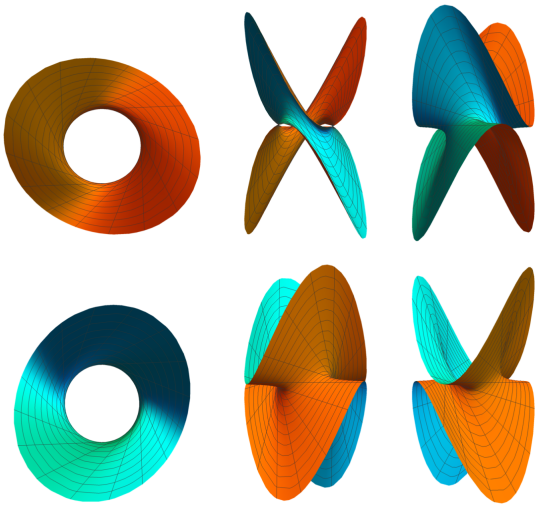

Figure 3. The halfway $n = 2$ surface at the points D_0 (top), and D_2 (bottom), with $t = -3/2$ (top), $t = +3/2$ (bottom), and $q = 2/3$, the pairs being viewed from different angles.

7. Inversion of the sphere

The sphere S^2 is given by $|\overline{R}|^2 = X^2 + Y^2 + Z^2 = R^2$, where $R > 0$ is a constant radius. We can give a periodic parametrization by $\phi \in [-\pi, \pi]$ (periodic) and by $\theta \in [-\pi/2, \pi/2]$ using $X = R\cos\theta\cos\phi$, $Y = R\cos\theta\sin\phi$, $Z = R\sin\theta$. We can map $\phi = \phi$, $h = \omega\sin\theta\cos^n\theta$

onto the cylinder, where $\omega > 0$. We can map the cylinder as

$$x' = x(\xi + \eta(x^2 + y^2))^{-\kappa}$$
$$y' = y(\xi + \eta(x^2 + y^2))^{-\kappa}$$
$$z' = z/(\xi + \eta(x^2 + y^2)),$$

where x, y, and z are as defined in the generalized time-dependent parametrization, for some $\xi, \eta \leq 0$, and $\kappa = (n-1)/2n$. We have

$$x'' = x' e^{yz'}/(\alpha + \beta(x'^2 + y'^2)),$$
$$y'' = y' e^{yz'}/(\alpha + \beta(x'^2 + y'^2)),$$
$$z'' = \frac{\alpha - \beta(x'^2 + y'^2)}{\alpha + \beta(x'^2 + y'^2)} \frac{e^{yz'}}{\gamma} - y^{-1} \frac{\alpha - \beta}{\alpha + \beta},$$

where $\alpha, \beta \leq 0$ and $\gamma = 2\sqrt{\alpha\beta}$. The geometric mean radius for this inversion sphere is then γ^{-1}. Let's consider the open wormhole, in this case, we would have $\xi = 1$, $\eta = 0$, $a = 1$, and $\beta \to 0$. Note that $h \to \pm\infty$ have a smooth mapping onto $(0, 0, -\sqrt{\alpha/\beta}(\alpha + \beta))$ at $x, y \to \infty$, $z \to 0$. This is a D_1 point at $n = 2$. Closing the wormhole then requires $\eta, \beta > 0$, with α, β, ξ, η dependent on t. We need $\beta = 1$, $a = 0$, $\xi = 0$, and $|t| > 1$ for the final step of the inversion of the xy plane:

$$x'' = x'/(x'^2 + y'^2),$$
$$y'' = y'/(x'^2 + y'^2),$$
$$z'' = -z'.$$

This can be equivalently expressed as the following:

$$x'' = \frac{\eta^\kappa x}{(x^2 + y^2)^{1-\kappa}},$$
$$y'' = \frac{\eta^\kappa y}{(x^2 + y^2)^{1-\kappa}},$$
$$z'' = -\frac{z/\eta}{x^2 + y^2}.$$

This completes the process of eversion. We have the complete eversion map:

$$(\theta, \phi) \to (h, \phi) \to \overline{r} = (x, y, z) \to \overline{r'} = (x', y', z') \to \overline{r''} = (x'', y'', z'').$$

This process almost created a sphere, but it is not fully rounded, and it is distorted. However, many interesting surfaces were obtained in this process, including Boy's surface, shown below.

In the final stage, after obtaining $\alpha = 0$, $\beta = 1$, and $\xi = 0$ at $|t| > 1$, consider parametrizing with $\lambda \in [0, 1]$ to get

$$x = (t(1 - \lambda + \lambda \cos^n \theta) \cos \phi - \lambda\omega \sin\theta \sin\phi)/\cos^n \theta,$$
$$y = (t(1 - \lambda + \lambda \cos^n \theta) \sin \phi + \lambda\omega \sin\theta \sin\phi)/\cos^n \theta,$$

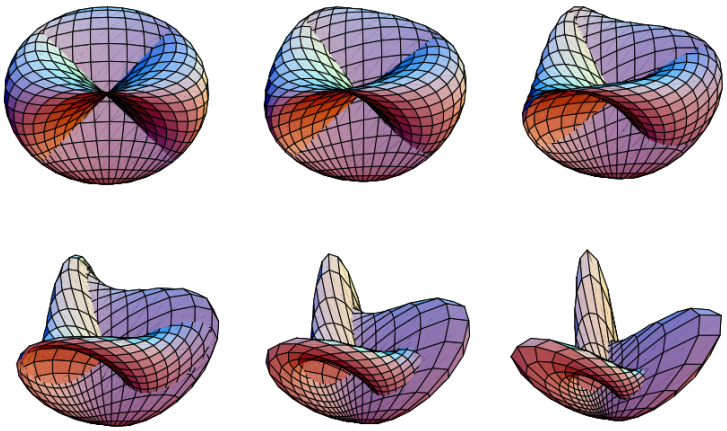

Figure 4. Boy's surface for $n = 3$ with $\xi = \eta = 1$, $\omega = 2$, $\alpha = 1$, and $\beta = 1/4$.

which then yields the following:

$$x'' = \eta^\kappa \cos\theta \frac{t(1-\lambda+\lambda\cos^n\theta)\cos\phi - \lambda\omega\sin\theta\sin\phi}{(t^2(\lambda\cos^n\theta+(1-\lambda))^2+\lambda^2\omega^2\sin^2\theta^{1-\kappa}},$$
$$y'' = \eta^\kappa \cos\theta \frac{t(1-\lambda+\lambda\cos^n\theta)\sin\phi + \lambda\omega\sin\theta\cos\phi}{(t^2(\lambda\cos^n\theta+(1-\lambda))^2+\lambda^2\omega^2\sin^2\theta^{1-\kappa}}$$

for $\lambda \in [0,1]$ as indicated earlier. Therefore, the following result, a growing function of $\cos^2\theta$, is

$$x''^2 + y''^2 = \eta^{2\kappa}\cos^2\theta(t^2(\lambda\cos^n\theta+(1-\lambda))^2+\lambda^2\omega^2\sin^2\theta)^{-1/n}.$$

We can plug

$$z = \lambda(\omega\sin\theta(\sin n\phi - qt)/\cos^n\theta - (t/n)\cos n\phi) - (1-\lambda)\eta^{1+\kappa}t|t|^{2\kappa}\sin\theta/\cos^{2n}\theta$$

into the final xy plane inversion equations from earlier. Thus, the mapping is smooth, and for $\lambda = 1$, we can recover the previous step, and $\lambda = 0$ is the final sphere with radius $R = \eta^\kappa|t|^{-1/n}$. [BB19] This completes the process of sphere eversion.

References

[BB19] Adam Bednorz and Witold Bednorz. Analytic sphere eversion using ruled surfaces. *Differential Geometry and its Applications*, 64:59–79, 2019.

[Sma59] Stephen Smale. A classification of immersions of the two-sphere. *Transactions of the American Mathematical Society*, 90(2):281–290, 1959.

[Sul02] John M Sullivan. Sphere eversions: from smale through "the optiverse". In *Mathematics and art*, pages 201–212. Springer, 2002.